Alignment dependence of high-order harmonic generation from N_2 and O_2 molecules in intense laser fields

XiaoXin Zhou,[1,2] X. M. Tong,[1] Z. X. Zhao,[1] and C. D. Lin[1]

[1]*J. R. Macdonald Laboratory, Physics Department,Kansas State University, Manhattan, Kansas 66506, USA*

[2]*College of Physics and Electronic Engineering, Northwest Normal University, Lanzhou, Gansu 730070, People's Republic of China*

The strong field approximation is used to investigate the harmonic generation of aligned N_2 and O_2 molecules. It is shown that the angular dependence of the yields of high-order harmonic generation from N_2 and O_2 molecules are different, which can be attributed to the orbital symmetry of the outmost electrons. The theory is applied to study the angular dependence of harmonic generation from recent pump-probe experiments where the pump pulse was used to produce the time-dependent partial alignment of molecules and the probe pulse was used to generate high-order harmonics. Good agreement with the experiments was found.

I. INTRODUCTION

The high-order harmonic generation (HHG) of atoms or molecules in intense laser fields is a subject of great research interest owing to its potential as a desk-top extreme ultraviolet (XUV) light source [1,2] and for the production of attosecond pulses [3,4]. While HHG has been well studied for atoms both theoretically and experimentally, much less has been done for molecules. The general features of HHG from atoms or molecules are similar: a steep drop in intensity in the low order, followed by a plateau region of nearly constant strength, and then a sharp drop beyond the cutoff. However, the details are different—especially the relative strength of the HHG and the location of the cutoff. By comparing atoms with molecules of nearly identical binding energies, Shan *et al.* [5] observed that the HHG cutoff of O_2 molecules is extended to higher order in comparison to its companion atom, Xe. No such extension was found for N_2 in comparison to its companion atom, Ar. According to the molecular tunneling ionization theory (MO-ADK) [6], the difference in O_2 and N_2 in HHG cutoff can be attributed to the fact that tunneling ionization rates depend critically on the wave function of the highest occupied molecular orbital (HOMO), in particular, their orbital symmetry. These orbital symmetries determine decisively how the ionization rates depend on the alignment of the molecules with respect to the direction of the laser's polarization. Since tunneling ionization is the precursor, that is, the first step in the three-step model for the harmonic generation [7], it is generally expected that the HHG yield would depend on the alignment of molecules as well.

Glimpse of such dependence has been found in experiments. Shan *et al.* [8] observed significant difference in the ellipticity dependence of HHG between O_2 and N_2. They attributed the difference to the ungerade vs the gerade HOMO orbitals of the two molecules, respectively. In their interpretation, the symmetry of the HOMO was not correctly represented, however. The effect of molecular alignment on HHG has also been studied by Marangos and co-workers [9–12] recently. They measured the HHG yield of H_2, N_2, CO_2, and CS_2 by a 70 fs high intensity laser in the presence of a weak long aligning laser. They found in general that the yield is enhanced in comparison to the case when the aligning laser is not present. To interpret their observations, they carried out restricted one-dimensional and two-dimensional model calculations. The calculations were found to have only limited success [11,12]. More recently, Itatani *et al.* [13] measured the HHG yield of N_2 and O_2 in a pump-probe arrangement: a weak short pulse was first used to create the field-free time-dependent dynamic alignment of molecules. A second intense short pulse is used to generate high-order harmonics at the short time interval when the molecules are maximally aligned. The HHG yield is then determined for different angles between the polarization direction of the probe laser with respect to the pump laser. In separate experiments, this group [14] and Kaku *et al.* [15] measured the HHG yield vs the time delay between the pump and probe pulses and determined the variation of the average HHG yield with the time delay. The variation of the HHG yields versus time was found to follow closely the average alignment of the molecules for N_2 molecules but not for O_2 molecules.

Theoretically, the alignment dependence of HHG can be obtained by calculating the dipole moment of molecules in the presence of laser fields, by solving the time-dependent Schrödinger equation. Even with a simplified one-electron model by including only the electron in the HOMO orbital of each molecule, such calculations [11,12] are still too time consuming to generate adequate data for comparison with experiments. It is well known that the emission of HHG from atoms can be described by the semiclassical three-step model [7]. First, an electron is tunnelled from the atom, the released electron is accelerated by the oscillating laser field and may be driven back to recollide with the parent ionic core, finally high-harmonic photons are emitted when the high-energy electron is recombined with the ionic core. The semiclassical version of this model for HHG is given by Lewenstein *et al.* [16] and this model is commonly called Lewenstein model. In this paper, we extended the Lewenstein model to calculate HHG from molecules, and applied it to study the alignment dependence of N_2 and O_2 molecules measured in recent experiments. Since the molecules in these measurements are

only partially aligned, integration of the HHG yields over the angular distribution of the molecules has to be carried out in order to compare with experiments. The paper is arranged as following. In Sec. II, we present the explicit expressions for the calculation of harmonic generation from molecules in a linearly polarized laser field by using the the Lewenstein model. In Sec. III, we show the dependence of the HHG yields for N_2 and O_2 molecules with fixed orientation in space. By convoluting these yields with the angular distributions of molecules from a pump pulse, the calculated harmonic yields are compared to recent pump-probe experiments. It is shown that a good agreement has been achieved with such simple calculations. The drastic difference between N_2 and O_2 molecules was attributed to the orbital symmetry of these molecules. Finally, the paper concludes with a short summary.

II. THEORETICAL MODEL

The model of Lewenstein *et al.* [16] for the high order harmonic generation from atoms was based on the strong field approximation. This model was obtained by expanding the time-dependent wavefunction in terms of the basis functions of the atom, with the laser-atom interaction providing the transitions. By truncating the Hilbert space to include only the ground state and excluding all the other bound excited states, and further approximating the continuum states by the Volkov states, the time-dependent dipole moment for an atom in the laser field $E(t)$ was expressed as [16]

$$r_\mathbf{n}(t) = i \int dt' \int d^3 \mathbf{p} \, \mathbf{n} \cdot \mathbf{d}^*[\mathbf{p} - \mathbf{A}(t)] a^*(t)$$
$$\times \mathbf{E}(t') \cdot \mathbf{d}[\mathbf{p} - \mathbf{A}(t')] a(t') e^{-iS(\mathbf{p},t,t')} + \text{c.c.} \quad (1)$$

where the laser polarization direction is along $\mathbf{n}$ and c.c. stands for complex conjugate. In Eq. (1), $a(t)$ is the amplitude of the ground state, $\mathbf{d}[\mathbf{p} - \mathbf{A}(t)]$ is the transition dipole moment between the ground state and the continuum state, with $\mathbf{p}$ and $\mathbf{A}$ the canonical momentum and vector potential, respectively, and

$$S(\mathbf{p}, t, t') = \int_{t'}^{t} dt'' \left[\frac{1}{2} [\mathbf{p} - \mathbf{A}(t'')]^2 + I_p \right] \quad (2)$$

is the quasiclassical action, where I_p is the ionization potential of the atom.

Equation (1) has clear physical interpretation. First, $\mathbf{E}(t') \cdot \mathbf{d}[\mathbf{p} - \mathbf{A}(t')] a(t')$ describes the amplitude of ionization by the laser field at time t'. The continuum electron propagates in the laser field from t' to t and acquires a phase factor $e^{-iS(\mathbf{p},t,t')}$. Finally, the electron recombines with the ion at time t with the probability amplitude $\mathbf{n} \cdot \mathbf{d}^*[\mathbf{p} - \mathbf{A}(t)] a^*(t)$. In Eq. (1), $a(t)$ was introduced to include the ground state depletion. After performing integration over $\mathbf{p}$ by the saddle point method, the time-dependent dipole matrix element reads
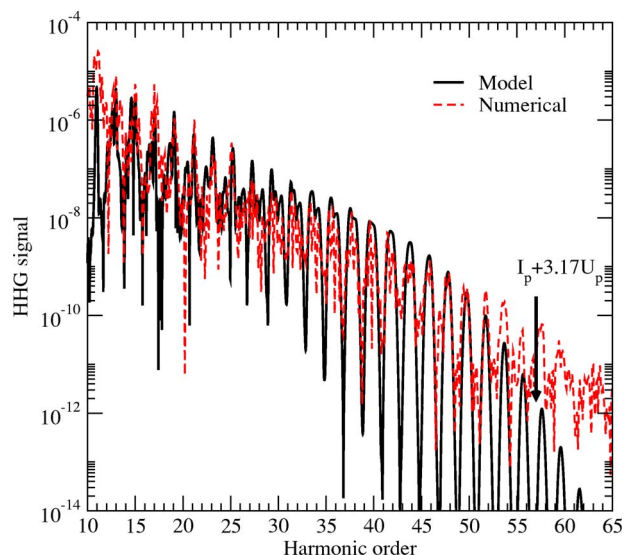

FIG. 1. (Color online) Comparison of high-order harmonic signals from atomic hydrogen calculated from Lewenstein model and from solving the time-dependent Schrödinger equation.

$$r_\mathbf{n}(t) = i \int_0^\infty d\tau \left(\frac{\pi}{\epsilon + i\tau/2} \right)^{3/2} \mathbf{n} \cdot \mathbf{d}^*[\mathbf{p}_{st}(t,\tau) - \mathbf{A}(t)] a^*(t)$$
$$\times \mathbf{E}(t-\tau) \cdot \mathbf{d}[\mathbf{p}_{st}(t,\tau) - \mathbf{A}(t-\tau)] a(t-\tau) e^{-iS_{st}(t,\tau)} + \text{c.c.}$$
$$(3)$$

where $\mathbf{p}_{st}(t,\tau) = \int_{t-\tau}^{t} \mathbf{A}(t'') dt'' / \tau$ is the momentum at the stationary point of the action, and ϵ is a small positive constant. In order to establish to what extent the Lewenstein model is valid, we carried out the calculation of HHG for atomic hydrogen by using the Lewenstein model and by directly solving time-dependent Schrödinger equation numerically [17]. In our calculation, we took the laser field to be a Gaussian pulse of 35 fs duration full width half maximum (FWHM), peak intensity $I = 4 \times 10^{14}$ W/cm^2, and mean wavelength $\lambda = 800$ nm. The results for hydrogen atom are shown in Fig. 1, in which the results predicted from the Lewenstein model are normalized to the ones from the *ab initio* calculation so they agree in the plateau region globally. This figure shows that overall the results from the two methods agree quite well. Above the cutoff position, the HHG from the numerical solution does not drop off quickly due to the HHG's were calculated from the length form [17] which is known to be less accurate in this region.

The Lewenstein model can clearly be extended to high order harmonic generation from aligned molecules. In this case, *ab initio* calculations of HHG from molecules are practically impossible except for a few very limited calculations [18–21]. To answer the questions of the alignment dependence of HHG for molecules, we thus chose to use the Lewenstein model to perform the calculation and focus only on harmonics in the plateau region. In the calculation, the molecule and the laser's polarization are chosen to be on the y-z plane, with the axis of the molecule being along the z axis. The polarization of the laser makes an angle θ with respect to the molecular axis. The time-dependent dipole mo-

ment Eq. (3) then takes the following form for molecules:

$$r(t) = i \int_0^\infty d\tau \left(\frac{\pi}{\epsilon + i\tau/2} \right)^{3/2} \{ \sin^2 \theta \, d_y^*(t) d_y(t - \tau)$$

$$+ \cos^2 \theta \, d_z^*(t) d_z(t - \tau) + \sin \theta \cos \theta [d_y^*(t) d_z(t - \tau)$$

$$+ d_z^*(t) d_y(t - \tau)] \} e^{-iS_{st}(t,\tau)} a^*(t) a(t - \tau) + \text{c.c.}, \qquad (4)$$

where d_y and d_z are the y and z components of the dipole moment of the molecule. The components of the molecular dipole moment are calculated using the ground state wave function of the molecule at the equilibrium distance and the final state wave functions approximated by the plane Volkov states, according to the Lewenstein model. In order to consider the depletion of the molecular ground state, its amplitude was approximated by $a(t) = \exp[-i\int_{-\infty}^t W(t')/2 dt']$, here the ionization rate $W(t')$ was evaluated using the tunneling ionization rate for molecules (the MO-ADK theory) [6]. Note that the tunneling ionization rates calculated using the MO-ADK theory have explicit alignment dependence [22]. Because the wave functions of N_2 and O_2 molecules have different symmetry, the ionization rates have different behavior with respect to the alignment of the molecular axis. The wave function of a diatomic molecule can be expressed in terms of basis functions on the two atomic centers

$$\Psi(\mathbf{r}) = \sum_i [a_i \phi_i(\mathbf{r} - \mathbf{R}/2) + b_i \phi_i(\mathbf{r} + \mathbf{R}/2)], \qquad (5)$$

where $\mathbf{R}$ is the vector between the two nuclei. For wave functions calculated from quantum chemistry codes, the basis functions are typically of the form

$$\phi_i(\mathbf{r}) = x^{n_{x_i}} y^{n_{y_i}} z^{n_{z_i}} e^{-\xi_i(x^2 + y^2 + z^2)}. \qquad (6)$$

We only need to consider d_y and d_z:

$$d_{y_i} = \frac{1}{(2\pi)^{3/2}} \int_{-\infty}^\infty e^{-i(p_x x + p_y y + p_z z)} y \phi_i(\mathbf{r}) dx \, dy \, dz, \qquad (7)$$

and a similar equation for d_z. The electronic wavefunctions of molecules in Eq. (7) were obtained from the GAMESS code [23]. In Eq. (5), there are two types of expansion coefficients for homonuclear molecules: one for antisymmetric mixing, $a_i = -b_i$, and another for symmetric mixing, $a_i = b_i$. For antisymmetric mixing, the Fourier transform has the form

$$\Psi^a(\mathbf{p}) = \sum_i \int a_i [\phi_i(\mathbf{r} - \mathbf{R}/2) - \phi_i(\mathbf{r} + \mathbf{R}/2)] e^{i\mathbf{p}\cdot\mathbf{r}} \, d^3\mathbf{r}$$

$$= 2i \sin(\mathbf{p} \cdot \mathbf{R}/2) \sum_i a_i \phi_i(\mathbf{p}) \qquad (8)$$

and for symmetric mixing:

$$\Psi^s(\mathbf{p}) = \sum_i \int a_i [\phi_i(\mathbf{r} - \mathbf{R}/2) + \phi_i(\mathbf{r} + \mathbf{R}/2)] e^{i\mathbf{p}\cdot\mathbf{r}} \, d^3\mathbf{r}$$

$$= 2 \cos(\mathbf{p} \cdot \mathbf{R}/2) \sum_i a_i \phi_i(\mathbf{p}), \qquad (9)$$

where $\phi_i(\mathbf{p})$ is the Fourier transform of wave function in Eq. (6). The dipole moment has similar form

$$d_y^a = 2i \sin(\mathbf{p} \cdot \mathbf{R}/2) \sum_i a_i d_{y_i}, \qquad (10)$$

$$d_y^s = 2 \cos(\mathbf{p} \cdot \mathbf{R}/2) \sum_i a_i d_{y_i}. \qquad (11)$$

Meanwhile, d_z has similar expressions. Once the time-dependent induced dipole moment is calculated from Eq. (4), its Fourier transform is used to obtain the angular dependence of the high-order harmonic spectra.

It is clear that Eq. (3) can be extended to polyatomic molecules as well. Experimentally, the angular dependence of the high-order harmonic spectra can be measured indirectly by the pump-probe technique. This is achieved by exposing the molecules to a short weak pulse to create a rotational wave packet. This wave packet rephrases at a later time and the molecules are strongly aligned periodically at intervals separated by their fundamental rotational period. Then, when the molecules are maximally aligned, a more intense laser pulse was used to generate high-order harmonics. For a short weak laser pulse, the alignment, or more explicitly, the time evolution of the angular distributions of an ensemble of homonuclear diatomic molecules, can be calculated by solving the time-dependent Schrödinger equation of a rigid rotor in a pump laser field. The validity of such a model has been tested experimentally [24]. A simple parameter that has been used to measure the degree of alignment of such an ensemble of molecules is $\langle \cos^2 \theta \rangle$ where the bracket means an ensemble average over the angular distribution of the molecules. If $\langle \cos^2 \theta \rangle$ is at the maximum, at the time of full or half rotational revivals, there are more molecules aligned in the laser polarization direction. Such favorable alignment lasts for tens of femtoseconds and a probe laser is used to generate HHG from these highly aligned molecules. We tested the present calculations against the experiment of Itatani *et al.* for N_2, where a pump pulse of intensity 4×10^{13} W/cm^2, duration 30 fs, wavelength 800 nm, was used to align the molecules. In order to compare with experimental data, the time-dependent emission yield of the $(2n+1)$th order harmonics $g_{2n+1}(t)$ of these aligned molecules was calculated from

$$g_{2n+1}(t) = \int \rho(\theta,t) \bar{g}_{2n+1}(\theta) d\Omega, \qquad (12)$$

where $\rho(\theta,t)$ is the angular distribution of the molecules after the pump laser is over. For quantitative measure, we use $\bar{g}_{2n+1}$ to denote the intensity of the $(2n+1)$th order harmonics by integrating the intensity calculated between the $2n$th and $(2n+2)$th orders for the pure aligned molecules. If the polarization directions of the probe and the pump pulses are different, then the integration over the angular distribution of the aligned molecules does not have the cylindrical symmetry and two-dimensional integration is needed.

III. RESULTS AND DISCUSSION

We calculated the alignment dependence of HHG for N_2 and O_2 molecules. In our calculation the laser pulse takes the Gaussian form:
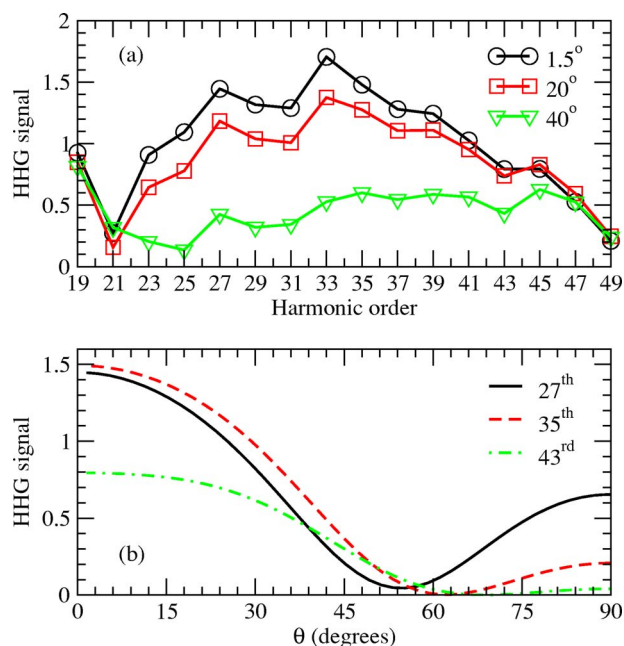
FIG. 2. (Color online) Alignment dependence of the HHG signals from N_2 calculated using the Lewenstein model. Laser pulse duration, 30 fs, peak intensity, 3×10^{14} W/cm², and mean wavelength, 800 nm.

$$E(t) = E_0 e^{-2 \ln 2 t^2 / \tau_w^2} \cos(\omega t) \qquad (13)$$

with pulse duration (FWHM) $\tau_w = 30$ fs, wavelength $\lambda = 800$ nm, and peak intensity $I = 3 \times 10^{14}$ W/cm² for N_2, and $I = 2 \times 10^{14}$ W/cm² for O_2. Figure 2 displays the results for N_2 molecules. In the upper panel, the HHG signals at different angles 1.5°, 20°, and 40° are shown. The strength of the HHG emission for N_2 molecules is maximum near 0° for harmonic orders in the plateau region between the 27th and the 45th. At larger angles, the harmonic yields decrease significantly. In the lower panel the angular dependence of the yield of selective 27th, 35th, and 43rd orders are given. In the plateau region, the angular dependence for different orders do not change much. The yield for each order has a minimum near 60°. This dependence is slightly different from the alignment dependence of the tunneling ionization rate of N_2 [22], which decreases monotonically with increasing angles according to the MO-ADK model. This difference can be attributed to the recombination process in the high-order harmonic generation. It is well known that the HHG is created in three steps: (a) tunneling ionization of the electron from the ground state; (b) propagation of the free electron in the oscillating laser field; and (c) emission of HHG by recombination of the rescattering electron with the ion back to the ground state. The first step happens in the asymptotic region and the alignment dependence of this process is well described by the MO-ADK theory [6]. For N_2, this angular dependence decreases monotonically from 0° to 90° [22]. The second step is relatively insensitive to the alignment because of the transverse spread of the wave packet of the returning electrons. The third recombination process happens in the inner region and angular dependence can arise from

the dipole matrix element, which in turn depends on the ground state molecular orbital near the equilibrium distance.

We can interpret the calculated angular dependence of HHG shown in Fig. 2(b) qualitatively. For N_2 molecules the ground state is a σ_g orbital. At large internuclear distances the molecular orbital consists of linear combinations of $2p_0$ atomic orbitals on the two centers with $a_i = -b_i$ [see Eq. (5)]. (Note the antisymmetric combination coefficients for σ_g orbital for the bonding orbital in N_2, instead of the symmetric ones stated in [25].) At smaller internuclear separations, hybridization is large and the actual σ_g molecular orbital does contain $2s$-type atomic orbitals from the two centers. For these s-type components, the mixing coefficients from the two centers are symmetric, i.e., $a_i = b_i$. According to Eqs. (10) and (11), the dipole matrix elements for the antisymmetric combination vanishes when the electron momentum is perpendicular to the internuclear axis, while for the symmetric combination the dipole matrix element has a local maximum there. We thus attribute the gradual rise in the HHG yields in Fig. 2(b) at larger angles to s-type atomic orbitals (instead of the p_0 type) in the ground state MO of N_2. From the actual MO wave functions used in our calculation, we found that the s type has a weight of 0.3, compared to the weight of 0.7 for the p_0 type. Since different orders of HHG probe different ranges of the momentum space ground state wave function, it may be anticipated that HHG from aligned molecules can provide a precise probe of molecular structure. On the other hand, it should be noted that the minimum predicted in Fig. 2(b) according to the present Lewenstein model could easily disappear due to contributions by electrons from other orbitals, or by deviations from the Lewenstein model itself. Thus experimental observation and/or precise *ab initio* calculations of the angular dependence of the HHG yields in the plateau region could be of interest for N_2 molecules.

In contrast to N_2, the results predicted for O_2 molecules are quite different (see Fig. 3). The HHG yields for a given alignment are nearly constant in the plateau region, but clearly they are very small when the molecules are aligned near the laser polarization direction. The yield reaches a maximum near about 50°–60° and then drops down at larger angles toward 90°. Note that the HOMO of O_2 molecules has π_g symmetry. The MO-ADK theory predicts that it has maximum tunneling ionization rates when the O_2 molecules are aligned at an angle of about 40°–45° from the direction of the laser's polarization, significantly smaller than the peak angles shown in the bottom frame of Fig. 3. Again, since recombination for the HHG occurs near the equilibrium distance while tunneling occurs where the electron is much farther away, the alignment angle where the ionization rate is maximum may differ somewhat from the angle where the HHG yield is maximum. For the π_g molecular orbital, it consists of $2p_1$-type atomic orbitals from the two centers with $a_i = -b_i$, i.e., antisymmetric mixing. The symmetric combinations would have to come from $3d_1$-type atomic orbitals. Actual π_g molecular orbitals calculated for O_2 shows there is little contribution beyond the $2p_1$ type. Thus the HHG for O_2 at 90° vanishes, as shown in Fig. 3(b).

The theoretical predictions of the angular dependence of the HHG yields presented above cannot be directly measured yet since it is not possible to freeze the rotational motion of
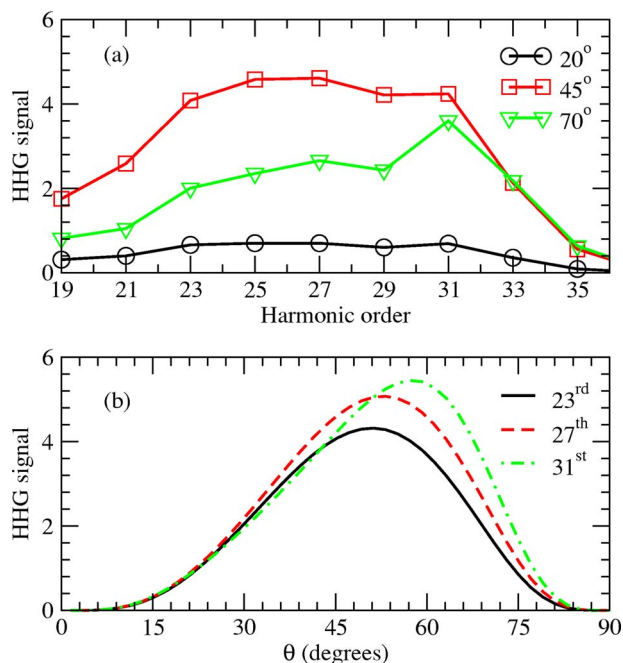
FIG. 3. (Color online) Alignment dependence of the HHG signals from O_2 calculated using the Lewenstein model. Laser pulse duration, 30 fs, peak intensity, 2×10^{14} W/cm^2, and mean wavelength, 800 nm.
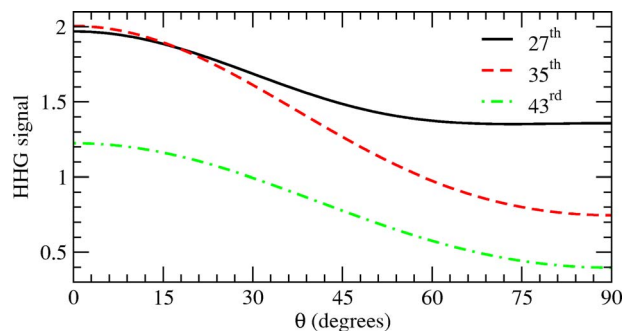

FIG. 4. (Color online) Dependence of the harmonic signals from N_2 with the angle between the polarization axes of the pump and probe lasers at the time when the molecules are maximally aligned.

molecules experimentally at finite temperature. The best one can do so far is to use a weak pump laser to partially align the molecules, and then use another probe laser to generate HHG from these molecules, and compare them to those without the presence of the pump laser. Partial alignment of molecules can be achieved by a short weak pulse to create a rotational wave packet. When the field-free wave packet rephases at full or half-full rotational periods, the molecules are instantaneously maximally aligned. In Itatani *et al.* [13], a second probe laser was used to generate high-order harmonics. By changing the polarization direction of the probe lasers, effectively the angular dependence of the HHG yields are determined. Since the maximum alignment by the pump laser achieved in this experiment is only modest, the theoretically predicted alignment dependence of HHG has to be convoluted with the angular distributions of the molecules from the pump pulse. By using the laser parameters from Itatani *et al.* [13], in a recent paper we have shown [26] that the dependence of the harmonic spectra from N_2 in the plateau region versus the angles between the pump and the probe lasers can indeed be explained by the Lewenstein model. The yields drop monotonically with increasing angle between the two polarizations. This behavior is by no means general. In fact, we have shown [26] that the dependence is entirely different for O_2 molecules. The HHG yield for all harmonics would peak when the polarizations of the two lasers are about 45° with respect to each other. No such experiment has been carried out for O_2 molecules yet.

To complement these earlier calculations, in Figs. 4 and 5 we show the angular dependence of individual harmonics for N_2 and O_2, respectively, in the plateau region. For N_2 the yield for each harmonic order decreases monotonically with

increasing angles, and for O_2 the yield for each harmonic order all peaks at about 45°. Note that these results are obtained by averaging over the partially aligned ensemble of molecules from the pump laser.

In another experiment, Itatani *et al.* [14] measured the harmonic yields versus time when the molecules are under the condition of free rotation after a short pump laser was used to generate the rotational wave packet. Since the angular distribution of the molecules changes continuously during the free rotation, a probe laser polarized in the same direction as the pump pulse would give time-dependent total HHG yield. In Fig. 6 we show the yield of the specific harmonic versus time for N_2 molecules, and compare it with the time evolution of the alignment of molecules, as qualitatively measured by the expectation values $\langle \cos^2 \theta \rangle$. From Fig. 6(a), it is clear that the time evolution of the different harmonics are about the same, and the dependence follows the alignment of the molecules shown in Fig. 6(b). This result is in agreement with the recent measurement of Itatani *et al.* [14]. For O_2 molecules, as shown in Fig. 7, the results are quite different from N_2. While the yield of each harmonic versus time does not change much for different harmonic order, they look quite different from the average alignment $\langle \cos^2 \theta \rangle$, as shown by the solid lines in Fig. 7(b). Since the peak of HHG yield occurs in the range of about 50°–60° [see Fig. 3(b)] for different harmonic order, a simple measure of such shift is to
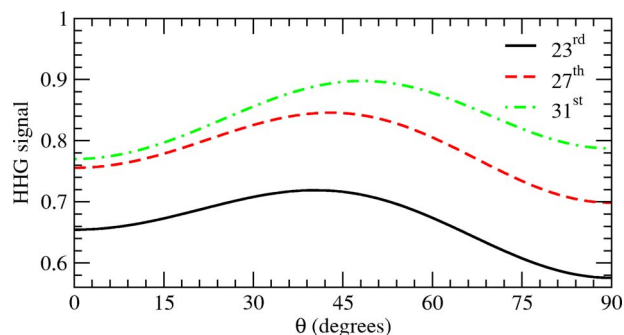

FIG. 5. (Color online) Dependence of the harmonic signals from O_2 with the angle between the polarization axes of the pump and probe lasers at the time when the molecules are maximally aligned. Laser parameters are identical to those used for N_2 except that the peak intensity is 2×10^{14} W/cm^2.
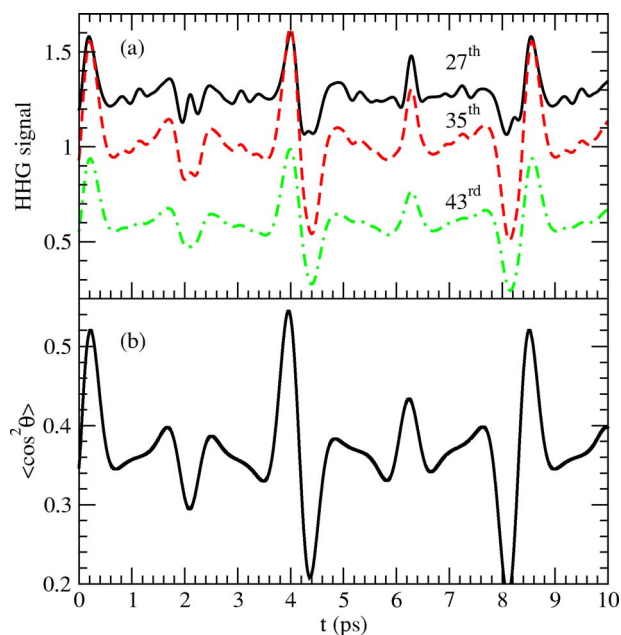
FIG. 6. (Color online) High-order harmonic yields generated by a probe pulse after the ensemble of molecules have been dynamically aligned by a pump laser pulse. The yield of each harmonic (a) versus time is shown to follow the average alignment $\langle \cos^2 \theta \rangle$ of the molecules (b). HHGs: the 27th(black), 35th(red), 43rd(green), for N_2 molecules.
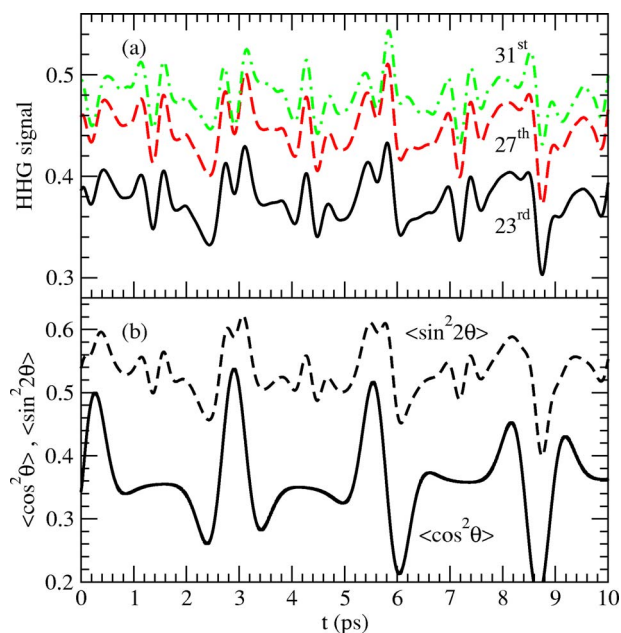

FIG. 7. (Color online) High-order harmonic yields generated by a probe pulse after the ensemble of molecules have been dynamically aligned by a pump laser pulse. The yield of each harmonic (a) versus time is shown not to follow the average alignment $\langle \cos^2 \theta \rangle$ of the molecules, but shifted by about 45°, as measured by $\langle \sin^2 2\theta \rangle$ (b). HHG signals: 23rd(black), 27th(red), 31st(green), for O_2 molecules.

compare it with $\langle \sin^2 2\theta \rangle$, which is shown as the dashed line in Fig. 7(b). Clearly this curve resembles the HHG yield results much better in Fig. 7(a). Note that the maxima and minima for each curve in Fig. 7(a) do not line up exactly with those in $\langle \sin^2 2\theta \rangle$, an indication of the shift of the maximum from 45° for each harmonic as seen in Fig. 3(b). The results presented here are again in agreement with the recent data of Itatani *et al.* [14] where only the sum of the harmonic yields with respect to time were compared.

IV. SUMMARY AND CONCLUSIONS

In this paper we showed that the Lewenstein model can be used to study the dependence of high-order harmonic yield in the plateau region versus the alignment angle of the diatomic molecules with respect to the direction of the linearly polarized laser pulse. Since full *ab inito* calculations on the alignment dependence of harmonic generation by molecules is still a formidable task, we have chosen the simpler Lewenstein model for this purpose, but with accurate ground state molecular wave functions. We have shown that the molecular structure, or more precisely, the orbital symmetry of the highest occupied molecular orbital, plays an essential role in determining the alignment dependence of HHG. Similar sen-

sitive dependence has been shown earlier for the tunneling ionization rates. While the prediction of the dependence of each harmonic with respect to the aligned angle of the molecular axis cannot be determined directly at present experimentally, the angular dependence of the harmonic yield from a partially aligned ensemble of molecules has been determined recently and we showed that the results are well explained by the present calculations based on the Lewenstein model. Our main conclusion is that the alignment dependence of HHG is determined mostly by the orbital symmetry of the HOMO of the molecules. This is just another example where the orbital symmetry of the outermost occupied electron plays an essential role in strong field physics. Future alignment dependence experiments on HHG should look for finer deviations from this general prediction, to establish the validity of the simple Lewenstein model, and identify possible effects of contributions from other shells.

[1] A. Rundquist, C. G. Durfee, Z. Chang, C. Herne, S. Backus, M. M. Murnane, and H. C. Kapteyn, Science **280**, 1412 (1998).

[2] R. A. Bartels, A. Paul, H. Green, H. C. Kapteyn, M. M. Murnane, S. Backus, I. P. Christov, Y. Liu, D. Attwood, and C. Jacobsen, Science **297**, 376 (2002).

[3] M. Drescher, M. Hentschel, R. Kienberger, G. Tempea, C. Spielmann, G. A. Reider, P. B. Corkum, and F. Krausz, Science **291**, 1923 (2001).

[4] M. Hentschel, R. Kienberger, C. Spielmann, G. A. Reider, N. Milosevic, T. Brabec, P. Corkum, U. Heinzmann, M. Drescher, and F. Krausz, Nature (London) **414**, 509 (2001).

[5] B. Shan, X. M. Tong, Z. Zhao, Z. Chang, and C. D. Lin, Phys. Rev. A **66**, 061401(R) (2002).

[6] X. M. Tong, Z. X. Zhao, and C. D. Lin, Phys. Rev. A **66**, 033402 (2002).

[7] P. B. Corkum, Phys. Rev. Lett. **71**, 1994 (1993).

[8] B. Shan, S. Ghimire, and Z. Chang, Phys. Rev. A **69**, 021404(R) (2004).

[9] R. Velotta, N. Hay, M. B. Mason, M. Castillejo, and J. P. Marangos, Phys. Rev. Lett. **87**, 183901 (2001).

[10] N. Hay, R. Velotta, M. Lein, R. de Nalda, E. Heesel, M. Castillejo, and J. P. Marangos, Phys. Rev. A **65**, 053805 (2002).

[11] R. de Nalda, E. Heesel, M. Lein, N. Hay, R. Velotta, E. Springate, M. Castillejo, and J. P. Marangos, Phys. Rev. A **69**, 031804(R) (2004).

[12] M. Lein, N. Hay, R. Velotta, J. P. Marangos, and P. L. Knight, Phys. Rev. A **66**, 023805 (2002).

[13] J. Itatani, J. Levesque, D. Zeidler, H. Niikura, H. Pepin, J. C. Kieffer, P. B. Corkum, and D. M. Villeneuve, Nature (London) **432**, 867 (2004).

[14] J. Itatani, D. Zeidler, J. Levesque, M. Spanner, D. M. Villeneuve, and P. B. Corkum, Phys. Rev. Lett. **94**, 123902 (2005).

[15] M. Kaku, K. Masuda, and K. Miyazaki, Jpn. J. Appl. Phys., Part 2 **43**, L591 (2004).

[16] M. Lewenstein, P. Balcou, M. Y. Ivanov, A. LHuillier, and P. B. Corkum, Phys. Rev. A **49**, 2117 (1994).

[17] X. M. Tong and S. I. Chu, Chem. Phys. **217**, 119 (1997).

[18] X. Chu and S. I. Chu, Phys. Rev. A **63**, 023411 (2001).

[19] D. A. Telnov and S.-I. Chu, Phys. Rev. A **71**, 013408 (2005).

[20] G. L. Kamta and A. D. Bandrauk, Phys. Rev. A **71**, 053407 (2005).

[21] B. Zimmermann, M. Lein, and J. M. Rost, Phys. Rev. A **71**, 033401 (2005).

[22] Z. X. Zhao, X. M. Tong, and C. D. Lin, Phys. Rev. A **67**, 043404 (2003).

[23] M. W. Schmidt *et al.*, J. Comput. Chem. **14**, 1347 (1993).

[24] I. V. Litvinyuk, K. F. Lee, P. W. Dooley, D. M. Rayner, D. M. Villeneuve, and P. B. Corkum, Phys. Rev. Lett. **90**, 233003 (2003).

[25] J. Muth-Bohm, A. Becker, and F. H. M. Faisal, Phys. Rev. Lett. **85**, 2280 (2000).

[26] X. X. Zhou, X. M. Tong, Z. X. Zhao, and C. D. Lin, Phys. Rev. A **71**, 061801(R) (2005).